

SUPPLEMENTAL INFORMATION

Supplemental Figure Legends

Figure S1 (relates to Figure 1)

Addition of an Unrelated Coiled-coil to the SUN Domain Supports KASH Binding.

(A) Schematic representation of SUN2 fragments and their derivatives. A luminal fragment of SUN2 was truncated stepwise to define the minimal requirements for KASH interaction. Note that also an unrelated coiled-coil (ucc) corresponding to a trimeric version of the GCN4 coiled-coil (Ciani et al., 2010) was used to replace the predicted coiled-coil region of SUN2 preceding the SUN domain.

(B) KASH binding of SUN2 and ucc-SUN2 constructs. The indicated purified His-tagged SUN2 derivatives were added to *E. coli* lysate to the same concentration (0.8 μ M for trimer) and incubated with immobilized zz-KASH2 or zz-KASH2 Δ as in Figure 1D. Bound proteins were retrieved and analyzed by SDS-PAGE followed by Coomassie staining. Loads in input and pulldown lanes correspond to 2.5% and 20% of the total, respectively.

Figure S2 (relates to Figures 2, 4)

Multiple Sequence Alignment of SUN Domains.

SUN domains from human SUN proteins and from highly diverged eukaryotes are shown. Secondary structure elements are shown above the sequence. The intramolecular disulfide bond is indicated by a yellow line. KASH contact sites are labeled. Red diamonds indicate pocket residues on SUN protomer 1, blue diamonds KASH-lid contacts. Colored circles indicate KASH binding sites on SUN protomer 2. The covalent link between SUN and KASH is indicated by a yellow dot.

Figure S3 (relates to Figure 3)

The SUN-KASH Disulfide Bridge Exist in vivo.

(A) HeLa cells transiently expressing GFP-tagged C-terminal fragments of Nesprins (GFP-Nesprin-1c, GFP-Nesprin-2c) or C-23S mutants were analyzed by SDS-PAGE under reducing and non-reducing conditions followed by Western blotting using anti-SUN1, anti-SUN2 or anti-GFP antibodies. In the non-reducing gel, disulfide-bridged SUN1 or SUN2 and GFP-Nesprins form the indicated high molecular weight complexes (a,c,e), which are destroyed under reducing conditions.

(B, C) Extracts of cells (A) were subjected to immunoprecipitation with anti-SUN1 (B) or anti-SUN2 (C) antibodies and isolated proteins analyzed by non-reducing SDS-PAGE followed by Western blotting using the indicated antibodies. Note that disulfide bridged

SUN-Nesprin wildtype complexes are precipitated. Note that the mutant Nesprins are not co-precipitated with SUN proteins under these conditions due to alkylation by NEM.

Figure S4 (relates to Figure 2)

Structural Homology with Lectins.

On the left, a SUN2 protomer with bound KASH2 peptide. On the right, Fucoslectin from European eel bound to fucose. Both proteins are shown in the same orientation. In both proteins, a metal cation organizes a loop that interacts with KASH and fucose, respectively. The loop is further held in place by an internal disulfide bond.

Figure S5 (relates to Figure 2)

Importance of SUN Trimerization and the Cation-loop for KASH-Binding.

(A) Point mutations were introduced in the SUN domain of human SUN2 in the backbone of His-tagged ucc-SUN2₅₂₂₋₇₁₇ to either distort trimeric organization (L536D, ΔR538, D542N) or the structure of the cation-loop (ΔN600). Wildtype ucc-SUN2₅₂₂₋₇₁₇ or the indicated mutants were co-expressed with MBP-KASH2 in *E. coli*. Interaction between MBP-KASH2 and the SUN domain variants was analyzed by a Ni-affinity pull-down assay of His-tagged SUN2. SDS-PAGE analysis of relevant fractions is shown. All mutants impaired binding of MBP-KASH2. Note that the D542N mutant of SUN2 appears to be compromised in folding, since it is largely insoluble.

(B) Analysis of wildtype SUN2₅₂₂₋₇₁₇ and the indicated mutants by CD spectroscopy. All proteins were purified and the unrelated coiled-coil removed by protease cleavage prior to CD analysis. The spectra do not reveal any gross variations and are typical for β-sandwich proteins, indicating that the point mutations do not affect the core fold of the SUN2 domain.

(C) The isolated SUN domain of SUN2 (SUN2₅₄₀₋₇₁₇) is a monomer. His-tagged SUN2₅₄₀₋₇₁₇ (calculated MW 23 kDa) was expressed in *E. coli*, purified by Ni-affinity chromatography and analyzed by gel filtration on a Superdex S200 HR10/300 column using Tris/HCl pH 7.5, 200 mM NaCl as running buffer. Calibration of the column relative to a molecular weight standard is indicated on top.

(D) Mutations disrupting the correct trimeric arrangement of SUN domains, which are deficient in KASH interaction (A), impair NE targeting of a SUN domain-dependent reporter construct *in vivo*. Wildtype SPAG4₁₋₁₈₉-SUN2₅₀₇₋₇₁₇-GFP, two point mutant derivatives (L536D, ΔR538) or SPAG4₁₋₁₈₉-SUN2₅₄₀₋₇₁₇-GFP, which lacks the trimeric coiled-coil region preceding the SUN domain, were expressed in HeLa cells. Cells were analyzed by confocal fluorescence microscopy.

Extended Experimental Procedures

DNA Constructs

DNA fragments coding for the C-terminal 29 aa of Nesprin-1 and Nesprin-2 (KASH1 and KASH2), or a deletion variant of KASH2 lacking the C-terminal 4 aa (KASH2 Δ), were amplified from HeLa cell cDNA by PCR. Coding sequences of all other KASH variants were cloned using oligonucleotides. All KASH constructs were cloned into pQE60-2z (Kutay et al., 1997). SUN2 fragments were amplified by PCR using pEGFP-N3-SUN2 (Turgay et al., 2010) as template. PCR fragments were cloned into pETDuet-1 (Novagen) to yield an N-terminally 6xHis-tagged fusion protein. Mutations were introduced into SUN2₃₃₅₋₇₁₇ and SPAG4₁₋₁₈₉-SUN2₅₀₇₋₇₁₇-GFP (Turgay et al., 2010) by QuikChange site-directed mutagenesis (Stratagene).

For crystallographic purposes, SUN2₅₂₂₋₇₁₇ was cloned similarly into pETDuet-1, but in addition a short coiled-coil fragment of GCN4 and a cleavage site for human rhinovirus 3C protease were inserted following the 6xHis-tag (Ciani et al., 2010). To co-express SUN2-KASH complexes, human Nesprin-1 (KASH1, residues 8769-8797) and Nesprin-2 (KASH2, residues 6857-6885) were cloned into the second cassette of the 6xHis-tri-GCN4 tagged SUN2 as 3C-cleavable maltose-binding-protein (MBP) fusions.

Recombinant Protein Expression and Purification

For protein binding assays, zz-KASH constructs were expressed in *E. coli* BLR(pRep4) for 4 hr at 37°C after induction with 0.5 mM IPTG. His-SUN2 constructs were expressed in *E. coli* BL21 Rosetta for 16 hr at 18°C after induction with 0.5 mM IPTG for SUN2₃₃₅₋₇₁₇ and SUN2₃₃₅₋₅₃₉, or with 0.1 mM IPTG for all other constructs. Cells were lysed by sonication in 50 mM Tris/HCl, pH 7.5, 200 mM NaCl. Lysates were cleared by ultracentrifugation (1 h, 50 000 rpm, Ti70, Beckman). SUN2 constructs were purified over Ni-NTA agarose (Qiagen), eluted in 50 mM Tris/HCl pH 7.5, 200 mM NaCl, 400 mM imidazole, and precipitated with 30% saturated (NH₄)₂SO₄ solution. Precipitates were dissolved in 50 mM Tris/HCl, pH 7.5, 200 mM NaCl, and residual ammonium sulfate was removed using illustra MicroSpin G-50 columns (GE Healthcare).

For crystallography, SUN2-KASH1 and SUN2-KASH2 were expressed in *E. coli* BL21(DE3) RIL strains (Stratagene). The bacterial cultures were grown at 30°C to an optical density (OD) of 0.6. Then, the culture was shifted to 18°C for 30 min and induced overnight with 0.2 mM IPTG. Apo-SUN2₅₂₂₋₇₁₇ expressing cells were resuspended in lysis buffer (50 mM potassium phosphate pH 8.0, 400 mM NaCl, 3 mM β -ME, 40 mM imidazole) and lysed. The lysate was supplemented with 1U/ml Benzonase (Sigma) and 1 mM PMSF, cleared by centrifugation, and loaded onto a Ni-affinity resin. After washing with lysis buffer, bound protein was eluted with elution buffer (10 mM Tris/HCl, 150 mM NaCl, 3 mM β -ME, 250 mM imidazole, pH 8.0). The eluted protein was purified by size exclusion chromatography on a Superdex S200 column (GE Healthcare) equilibrated in crystallization buffer (10 mM Tris/HCl pH 8.0, 150 mM NaCl, 0.1 mM EDTA and 1 mM DTT). After cleaving with 3C protease the protein was separated from the fusion tag by a second size exclusion step under identical conditions. SUN2-KASH1 and SUN2-KASH2 were purified using the protocol developed for apo-SUN2, except that reducing and chelating agents were omitted and elution as well as crystallization buffers contained 1 mM CaCl₂.

To allow selenium phasing, a second methionine was introduced into the SUN2522-717 sequence (L546M) using PCR mutagenesis. The seleno-methionine (SeMet)-derived protein was obtained using methionine-pathway inhibition as described before (Brohawn et al., 2008).

For the SUN-KASH pull-down experiment shown in Figure S4, the 6xHis-SUN2-MBP-KASH2 pairs were co-expressed in *E. coli* and Ni-purified under the conditions described for the preparation of the crystallographic samples.

In Vitro Binding Experiments

Per binding reaction, 15 μ l of IgG sepharose were saturated with zz-KASH derivatives by incubation in cleared lysate of *E. coli* expressing the respective construct. Beads were washed and added to binding reactions.

For binding of endogenous SUN proteins, 2×10^6 HeLa cells were lysed in 200 μ l RIPA buffer (50 mM Tris/HCl pH 7.5, 200 mM NaCl, 0.5% NP40, 0.1% DOC, 0.025% SDS) containing protease inhibitors (1 mM PMSF, 10 μ g/ml aprotinin, 10 μ g/ml leupeptin, 1 μ g/ml pepstatin A).

For binding of recombinant SUN2 constructs, purified proteins were added to 200 μ l 'empty' *E. coli* lysate supplemented with RIPA detergents (final buffer composition: 50 mM Tris/HCl, pH 7.5, 200 mM NaCl, 0.5% NP40, 0.1% DOC, 0.025% SDS). Alternatively (Figure 6A,B), cleared lysate of *E. coli* expressing recombinant SUN2₃₃₅₋₇₁₇ was used directly.

Samples were incubated for 4 hr at 4°C in an overhead shaker. Beads were washed and bound proteins were eluted with SDS sample buffer.

Protein Crystallization

Purified SUN2₅₂₂₋₇₁₇ and SeMet-derivatized SUN2(L546M) were concentrated to 15 mg/ml prior to crystallization. The apo-proteins crystallized in 16% (w/v) polyethylene glycol (PEG) 3350 and 200 mM potassium thiocyanate by the hanging drop vapor diffusion method in 2 μ l drops at 18°C. Rhombohedral crystals grew within 2-5 days with dimensions of 15 μ m³ x 15 μ m x 15 μ m. The co-purified SUN2-KASH1 complex was concentrated to 13 mg/ml and similarly-shaped crystals were obtained from 100 mM HEPES pH 7.4, 7% PEG 4000, 10% 1,6-hexandediol and 0.25% n-decyl- β -D-maltoside (DM). For the SUN2-KASH2 crystals, the complex was concentrated to 10 mg/ml and was set up in 100 mM HEPES pH 7.5, 200 mM ammonium acetate, 25% 2-propanol and 0.3% DM. All crystals were cryoprotected in the reservoir solution supplemented with 18% (v/v) glycerol. Data were collected at beamlines 24ID-C/-E at Argonne National Laboratory.

Structure Determination

Data reduction was carried out using HKL2000 (Otwinowski and Minor, 1997). The structure of apo-SUN2 was solved using single anomalous dispersion (SAD) data from the SeMet derivatized SUN2 L546M mutant. The AutoSol procedure from the PHENIX suite was used for phasing and initial refinement (Adams et al., 2010). The final model was refined against native data extending to 2.2 Å. Model building was carried out with

Coot (Emsley et al., 2010) and refinement was done with phenix.refine from the PHENIX suite. All residues were assigned including an additional Gly-Pro dipeptide at the N terminus, a remnant of the proteolytic cleavage site.

The SUN2-KASH1 and SUN2-KASH2 structures were subsequently solved by molecular replacement using apo-SUN2 as the search model. Model building was carried out with Coot and refinement was done with phenix.refine. Both complex models are complete for the SUN2₅₂₂₋₇₁₇ sequence. For the KASH1 and KASH2 peptides, the N-terminal residues 8769-8771 and 6857-6860, respectively, could not be positioned, presumably due to their flexibility in the crystal.

Analytical Ultracentrifugation

Purified SUN2₃₃₅₋₇₁₇ was gel-filtered in 10 mM Tris/HCl pH 8.0, 150 mM NaCl and 1 mM CaCl₂ immediately prior to the experiments. Analytical ultracentrifugation experiments were carried out with an Optima XL-A centrifuge using an An60Ti rotor. Samples for sedimentation equilibrium (110 µl sample or 120 µl buffer) were loaded into Epon-charcoal 6 channel centerpieces, fit with quartz windows, and spun at 7000 and 10000 rpm, respectively. Two concentrations (0.3 and 0.5 mg/ml) were analyzed. Reaching of the sedimentation equilibrium was monitored with Winmatch. Absorbance data was collected at 280 nm at 5 replicates per 1 nm step. Sedimentation equilibrium data were globally fitted with Ultrascan II (<http://ultrascan.uthscsa.edu>) with a single ideal species model.

Circular Dichroism

The experiments were carried out at 25°C using an Aviv Model 202 spectrometer. Spectra were recorded at 25 µM protein concentration in a cuvette with 0.1 mm optical pathlength. Spectra were recorded in 1 nm steps, averaged for 10 sec, and corrected for buffer baseline.

Cell Culture, Transfection and Microscopy

HeLa cells were maintained in DMEM containing 10% FCS, 100 U/ml penicillin, and 100 µg/ml streptomycin at 37°C and 5% CO₂. Transient transfection was performed using X-tremeGENE transfection reagent (Roche). 24 hr after transfection, cells were fixed with 1% PFA for 10 min and then washed with PBS. Coverslips were mounted on VectaShield (VectorLabs). Confocal images were acquired with a Leica TCS-SP1 microscope using a HCX PI APO lbd.BI. 40x, NA 1.25 oil immersion objective.

Analysis of DTT-sensitive disulfide bridges

HeLa cells were transiently transfected with plasmid DNA encoding GFP-Nesprin-1c (aa 8444-8797 of Nesprin-1 isoform 1, NP_892006.3), GFP-Nesprin-2c (aa 6555-6885 of Nesprin-2 isoform 1, NP_055995.4), or their mutant versions. After 48 hr, cells were harvested and treated with 20 mM N-ethyl maleimide (NEM). Cells were lysed in SDS sample buffer either without (non-reducing) or with 50 mM DTT (reducing). Lysates were analyzed by SDS-PAGE followed by Western Blotting.

References to Supplemental Information

- Adams, P.D., Afonine, P.V., Bunkoczi, G., Chen, V.B., Davis, I.W., Echols, N., Headd, J.J., Hung, L.W., Kapral, G.J., Grosse-Kunstleve, R.W., *et al.* (2010). PHENIX: a comprehensive Python-based system for macromolecular structure solution. *Acta crystallographica. Section D, Biological crystallography* **66**, 213-221.
- Brohawn, S.G., Leksa, N.C., Spear, E.D., Rajashankar, K.R., and Schwartz, T.U. (2008). Structural evidence for common ancestry of the nuclear pore complex and vesicle coats. *Science* **322**, 1369-1373.
- Ciani, B., Bjelic, S., Honnappa, S., Jawhari, H., Jaussi, R., Payapilly, A., Jowitt, T., Steinmetz, M.O., and Kammerer, R.A. (2010). Molecular basis of coiled-coil oligomerization-state specificity. *Proc. Natl. Acad. Sci. U. S. A.* **107**, 19850-19855.
- Emsley, P., Lohkamp, B., Scott, W.G., and Cowtan, K. (2010). Features and development of Coot. *Acta crystallographica. Section D, Biological crystallography* **66**, 486-501.
- Kutay, U., Izaurralde, E., Bischoff, F.R., Mattaj, I.W., and Gorlich, D. (1997). Dominant-negative mutants of importin-beta block multiple pathways of import and export through the nuclear pore complex. *EMBO J.* **16**, 1153-1163.
- Otwinowski, Z., and Minor, W. (1997). Processing of X-ray diffraction data collected in oscillation mode. *Methods Enzymol.* **276**, 307-326.
- Turgay, Y., Ungricht, R., Rothballer, A., Kiss, A., Csucs, G., Horvath, P., and Kutay, U. (2010). A classical NLS and the SUN domain contribute to the targeting of SUN2 to the inner nuclear membrane. *EMBO J.* **29**, 2262-2275.

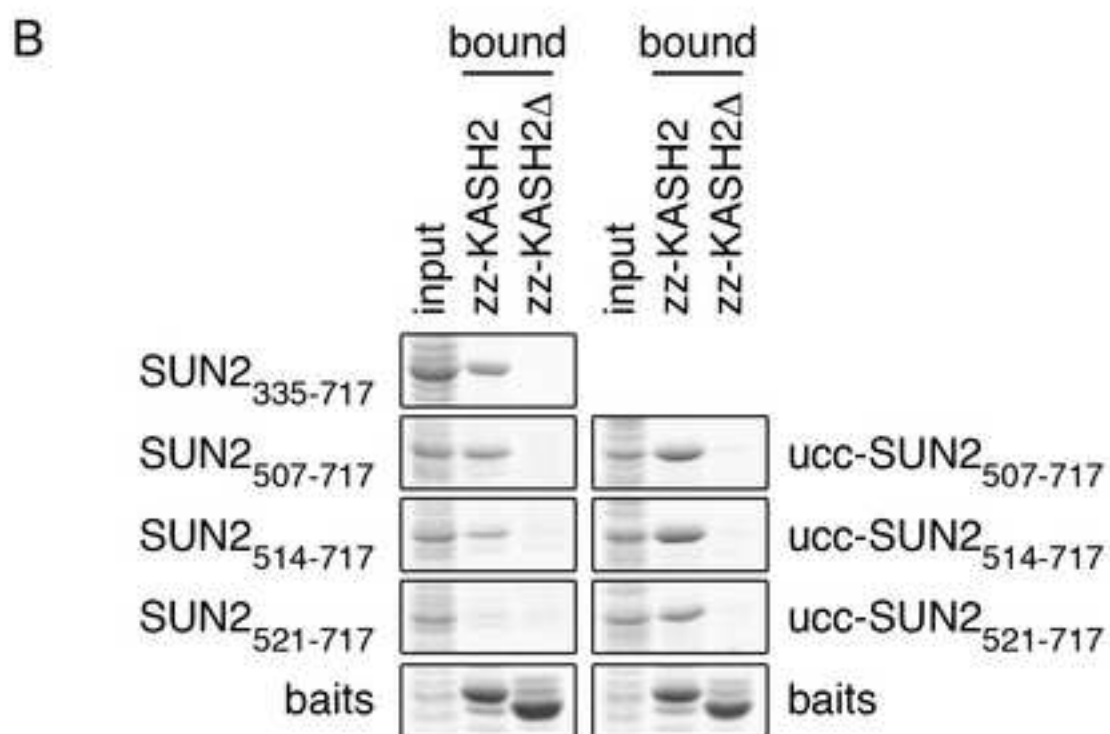
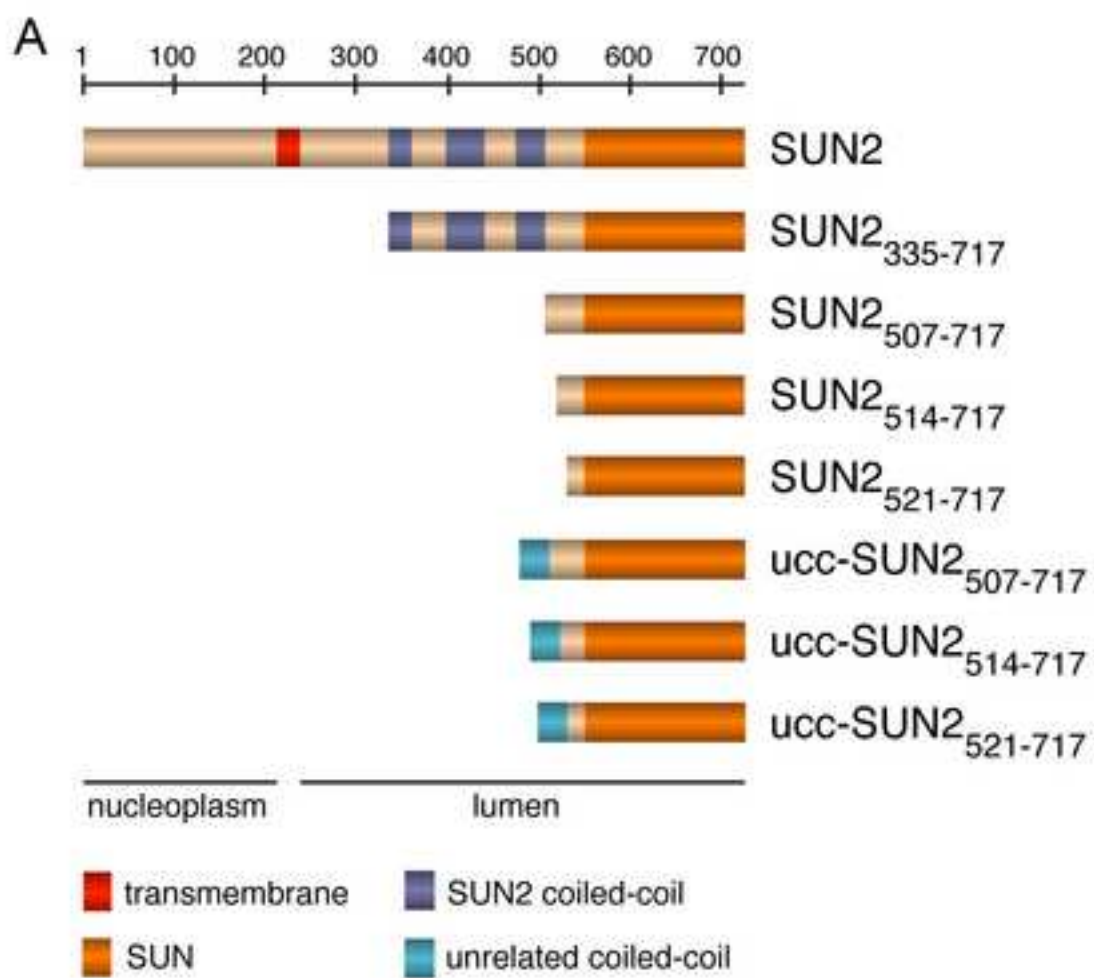


Figure S1

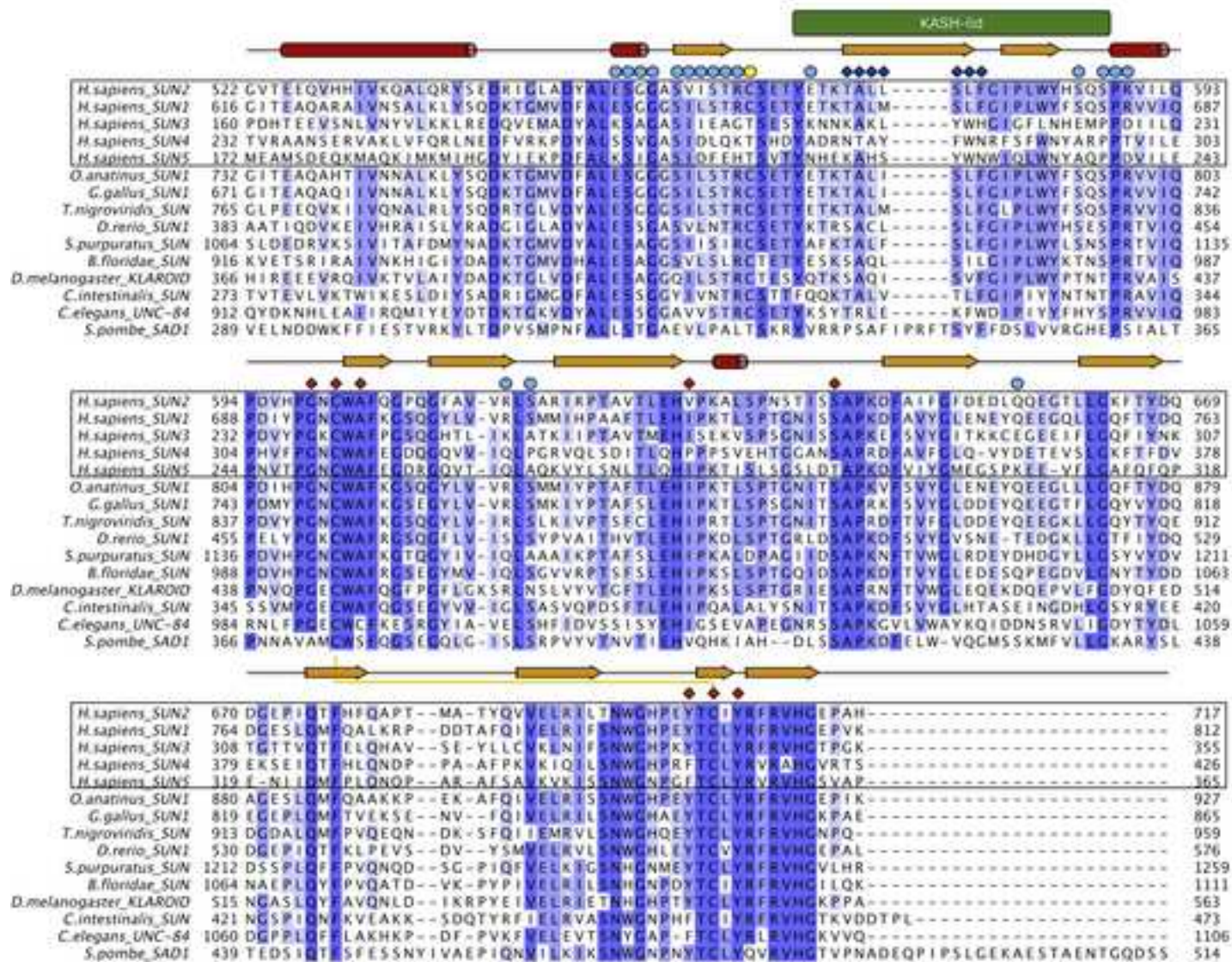
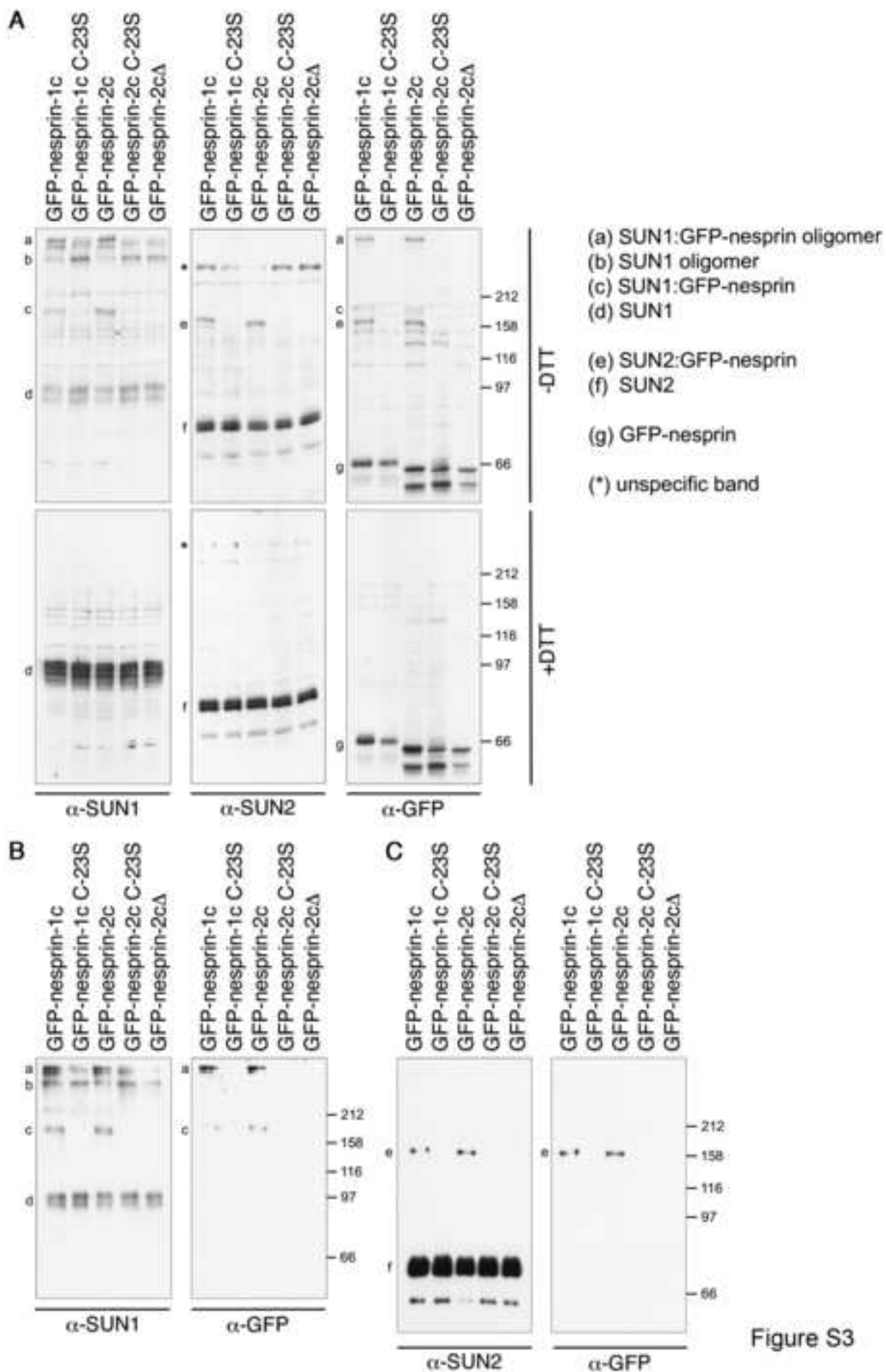
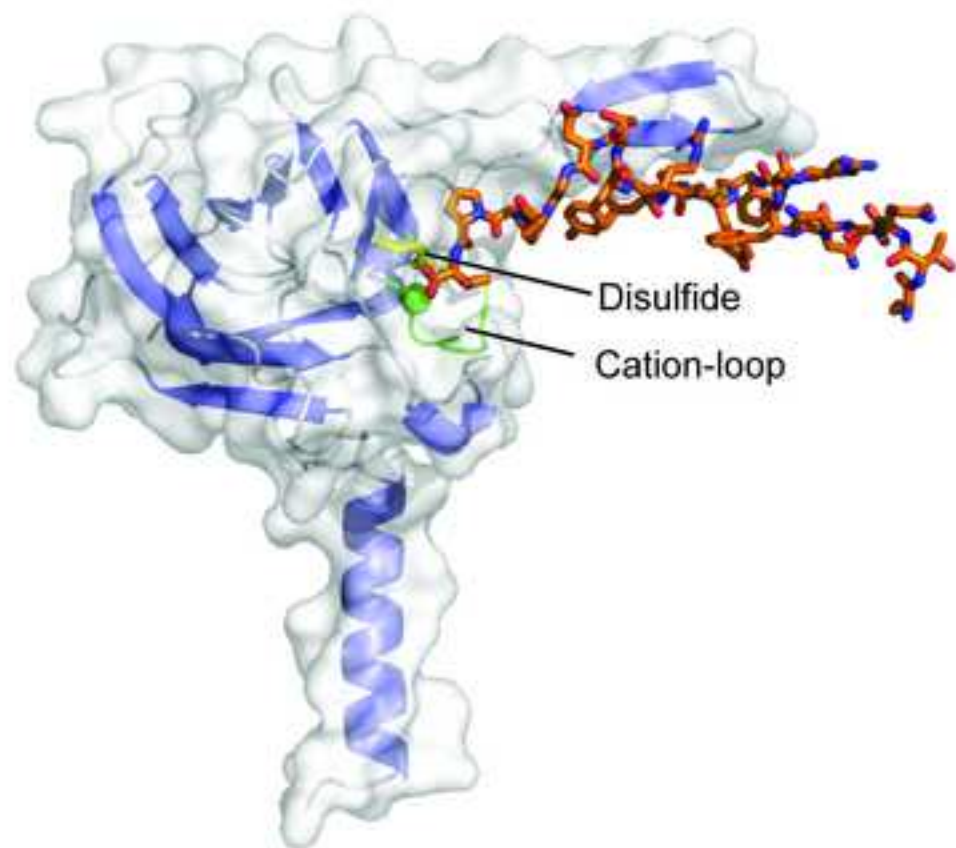


Figure S2



SUN2-KASH2



Fucolectin-Fucose

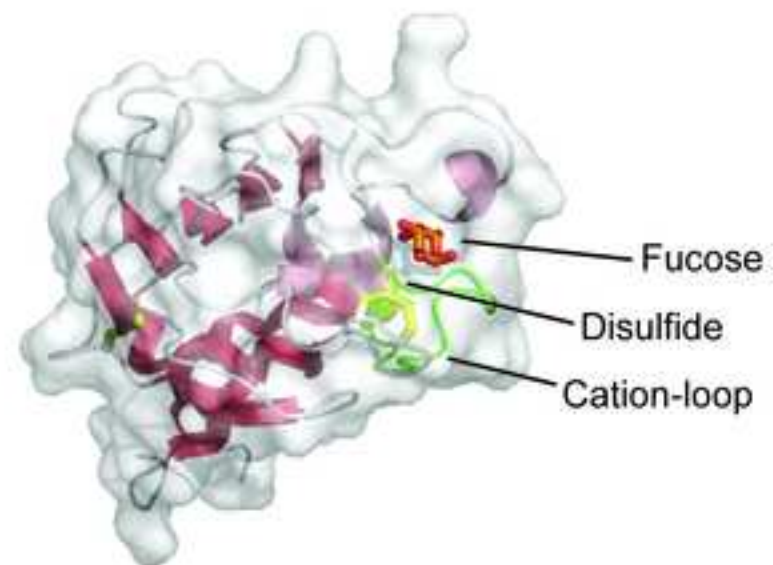


Figure S4

